

## **Supplementary Information**

### **Mechanistic Insight into Dendrite-SEI Interactions for Lithium Metal**

#### **Electrodes**

*Feng Hao, Ankit Verma and Partha P. Mukherjee\**

School of Mechanical Engineering, Purdue University, West Lafayette, IN 47907, USA

\*Correspondence: pmukherjee@purdue.edu

## 1. Dynamical Evolution during Li Plating

In our system, three processes are considered: surface desolvation of Li-ions from electrolyte into solid electrolyte interphase (SEI), Li-ion transport through the SEI layer, and Li reduction and growth on the anode surface. All the three processes can be well captured by the kinetic Monte Carlo (KMC) algorithm.<sup>1</sup> The detailed dynamical evolution of the system is described below.

Three rate constants: desolvation rate  $k_a$ , Li-ion diffusion rate  $k$ , and electrochemical reaction rate  $k_j$  (see the definitions in the manuscript). These rates are calculated for each lattice site, and the total rate needs to be obtained first.

For Li-ion desolvation,

$$k_1 = \sum_{j=1}^{N_1} k_a^j, \quad (\text{S1})$$

where  $k_1$  is the total desolvation rate of Li-ion, and  $N_1$  is the number of unoccupied lattice sites by Li-ions on the upper SEI surface.

For Li-ion transport through the SEI layer,

$$k_2 = \sum_{j=1}^{N_2} k^j, \quad (\text{S2})$$

where  $k_2$  is the total diffusion rate, and  $N_2$  is the number of Li-ions inside the SEI layer.

For the electrochemical reaction,

$$k_3 = \sum_{j=1}^{N_3} k_j^j, \quad (\text{S3})$$

where  $k_3$  is the total reaction rate, and  $N_3$  is the number of Li-ions at the anode-SEI interface.

Then, we have the total rate

$$k_{tot} = \sum_{j=1}^3 k_j, \quad (\text{S4})$$

Set a random number  $r_1$ , distributed on (0,1), multiplies it by  $k_{tot}$ , and steps through all the events, stopping at the first event for which the total rate of previously scanned events is large than  $r_1 k_{tot}$ .<sup>1</sup>

Thus, this event is selected to occur. The time step is estimated by a random number  $r_2$

$$\delta t = -\frac{1}{k_{tot}} \ln r_2, \quad (\text{S5})$$

The specific flow is illustrated in Figure S1.

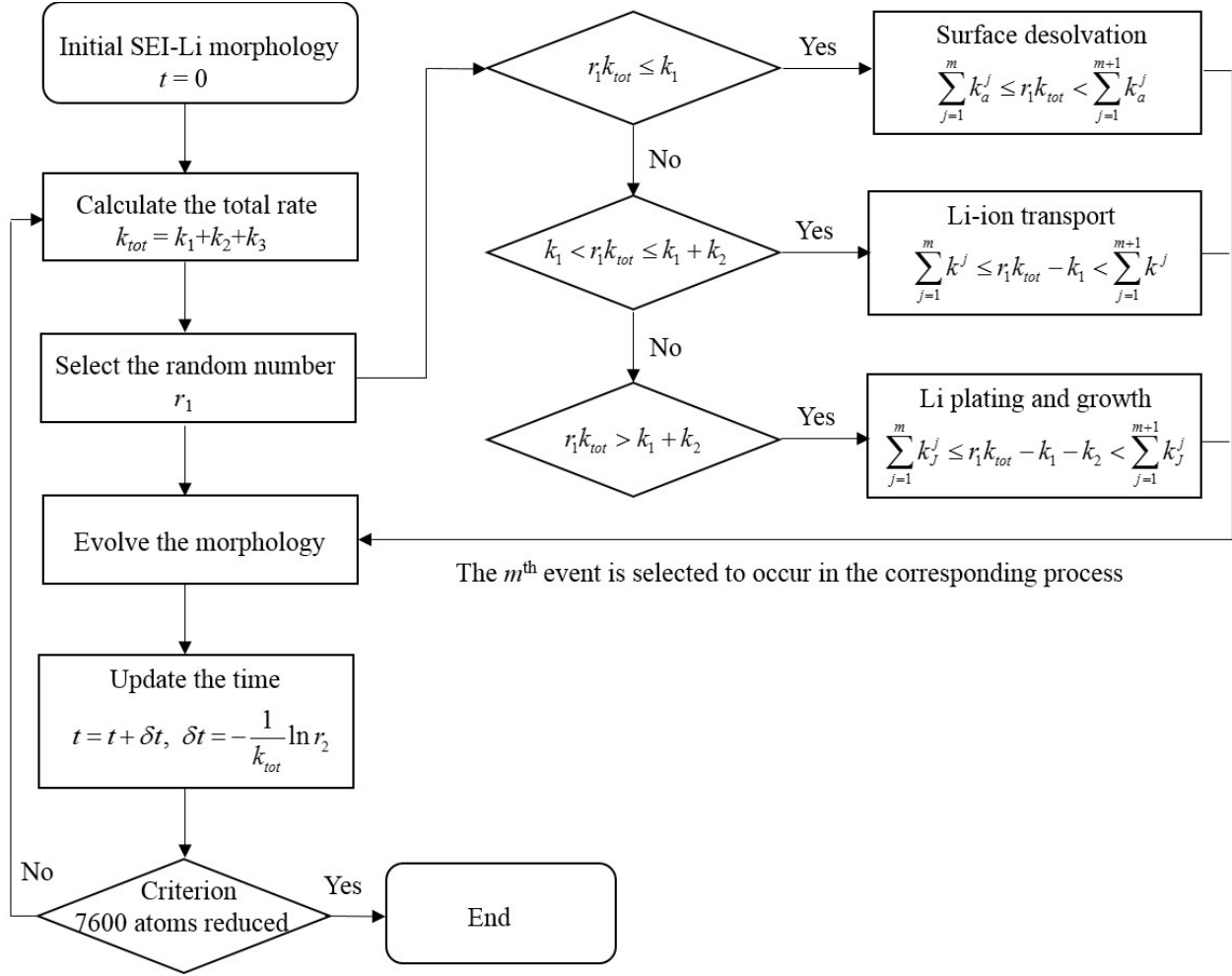


**Figure S1.** Schematic of the KMC procedure for the dynamical evolution.

## 2. Parameters Used in the Kinetic Model

Table 1S lists all the parameters used in the kinetic model, of which two parameters are discussed below.

*Li-ion diffusion barrier in the SEI layer  $E_a$ .* Depending on the materials in SEI, such as  $\text{Li}_2\text{CO}_3$ ,  $\text{Li}_2\text{O}$ , and  $\text{LiF}$ , the energy barrier can range from 0.15 eV to 0.73 eV.<sup>2, 3</sup> In our current model, we use a simple model for SEI: SEI is homogenous in the thickness direction. Here, we use

a value of 0.4 eV.

*Li-ion desolvation rate*  $k_a$ . It was reported that the activation energies for Li-ion desolvation reactions are 0.42-0.46 eV at the electrolyte-SEI interface.<sup>4</sup> In our study, we assume that Li-ion desolvation rate is  $1 \times 10^5 \text{ s}^{-1}$ . According to the Arrhenius expression ( $k_a = \nu \exp\left(\frac{-E_{act}}{k_b T}\right)$ , see  $\nu$ ,  $k_b$ , and  $T$  in Table 1S), the estimated activation energy is 0.43 eV in our model, which is consistent with the reported ones.<sup>4</sup>

**Table 1S.** Parameters used in the model.

Parameters		Values	Units	References
$\eta$	Local overpotential	0.1-0.3	V	
$i_0$	Exchange current density (Li/Li <sup>+</sup> )	5	mA cm <sup>-2</sup>	5, 6
$\alpha$ ( $\beta$ )	Charge transfer coefficients (Li/Li <sup>+</sup> )	0.7 (0.3)		5, 6
$E_a$	Li-ion diffusion barrier in SEI	0.4	eV	2, 3
$k_a$	Li-ion desolvation rate	$10^5$	s <sup>-1</sup>	4
$a$	Li lattice constant	3.5	Å	7
$R$	Gas constant	8.314	J mol <sup>-1</sup> K <sup>-1</sup>	
$F$	Faraday constant	96,487	C mol <sup>-1</sup>	
$N_a$	Avogadro constant	$6.022 \times 10^{23}$	mol <sup>-1</sup>	
$k_b$	Boltzmann constant	$1.38 \times 10^{-23}$	m <sup>2</sup> kg s <sup>-2</sup> K <sup>-1</sup>	
$T$	Operating temperature	300	K	
$\nu$	Pre-exponential factor	$2 \times 10^{12}$	s <sup>-1</sup>	1

In Figure 3 (in the manuscript),  $D_c/D$  is varied to describe the SEI inhomogeneity.  $D_c$  and  $D$  are determined by Li-ion diffusion barriers in SEI. Table 2S lists the corresponding diffusion barriers in the kinetic model for the varying  $D_c/D$ .

**Table 2S.** Diffusion barriers used in Figure 3.

$D_c/D$	$E_a$ in the center region (eV)	$E_a$ in the other regions (eV)
0.3	0.43	0.4
0.7	0.41	0.4
1.0	0.4	0.4
1.5	0.39	0.4
3.2	0.37	0.4

### 3. Theoretical Analysis of Li-ion Concentration Distribution

For the kinetic model, new Li-ions are added to the system from the SEI upper surface to compensate Li consumption at the Li metal-SEI interface. Thus, Li-ion concentration in the SEI layer is kept at  $c_0 = 1500 \text{ mol/m}^3$ , approximately 240 Li-ions in our system. We assume that the SEI layer has a thickness of  $h$ , with the upper surface ( $x = h$ ) and Li metal-SEI interface ( $x = 0$ ).

For our considered model, we have the conditions of Li-ion transport in the SEI layer

$$D \left. \frac{\partial c}{\partial x} \right|_{x=0} = -\frac{i}{F}, \quad (\text{S6})$$

$$D \left. \frac{\partial c}{\partial x} \right|_{x=h} = -\frac{i}{F}, \quad (\text{S7})$$

$$c(x, t = 0) = c_0, \quad (\text{S8})$$

where  $i$  is the current density (unit mA/cm<sup>2</sup>). The solution is expressed as<sup>8</sup>

$$c - c_0 = \frac{ih}{DF} \left\{ -\frac{x}{h} + \frac{1}{2} - 4 \sum_{n=1}^{\infty} \frac{1}{(2n-1)^2 \pi^2} e^{-(2n-1)^2 \pi^2 \frac{Dt}{h^2}} \cos \left[ (2n-1) \pi \frac{x}{h} \right] \right\}. \quad (\text{S9})$$

After a substantial period of plating, a stable concentration gradient through the SEI layer is formed, and the corresponding steady-state concentration distribution is reduced to

$$c - c_0 = \frac{ih}{DF} \left( -\frac{x}{h} + \frac{1}{2} \right). \quad (\text{S10})$$

Using  $i_L = 2c_0 DF / h$ , the above equation is rewritten as

$$\frac{c}{c_0} = \frac{i}{i_L} \left( 1 - 2 \frac{x}{h} \right) + 1. \quad (\text{S11})$$

Thus, the dimensional concentration profile (in the thickness direction) depends on the dimensional current density  $i/i_L$ .  $i$  is related to the overpotential applied to the system. In the manuscript, Figure 2 indicates that the results directly obtained from the kinetic model are in a good agreement with the theoretical results from Eq. (S11).

#### 4. Stress Analysis

Figure 2S illustrates the mechanism of Li plating induced stress. Because of the Li growth, the anode surface will move upwards. For uneven Li plating, the anode-SEI interface becomes rough, which generates stress in the SEI layer.

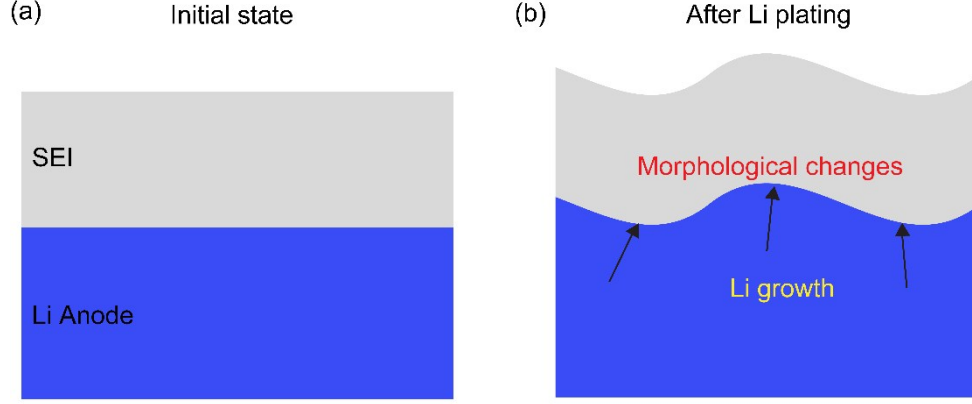


**Figure S2.** Schematic of Li growth at the anode-SEI interface, and the morphology changes generate stress.

Finite element method (FEM) is employed to analyze the deformation and stress of the SEI layer. For the SEI upper surface, the stress-free boundary condition is assumed, which is applicable to the conditions: SEI does not contact with the separator in battery or the force between SEI and separator is negligible. For the SEI bottom surface, the displacement field is obtained from the kinetic model, i.e. the movement of the anode-SEI interface. For the left and right boundaries, the periodic boundary condition (PBC) is applied, which implies that the two boundaries share the same physical field. Young's modulus and Poisson's ratio are assumed to be 10 GPa and 0.3, respectively.

For FEM, the basic equations are<sup>9</sup>

$$\mathbf{K}\mathbf{b} = \mathbf{P}, \quad (\text{S12})$$

$$\mathbf{K} = \sum_e \int_{V_e} \mathbf{B}^T \mathbf{D} \mathbf{B} dV, \quad (\text{S13})$$

$$\boldsymbol{\varepsilon} = \mathbf{B}\mathbf{b}^e, \quad (\text{S14})$$

$$\boldsymbol{\sigma} = \mathbf{D}(\boldsymbol{\varepsilon} - \boldsymbol{\varepsilon}_0) + \boldsymbol{\sigma}_0, \quad (\text{S15})$$



where  $\mathbf{K}$  is the global stiffness matrix of the element assemblage,  $\mathbf{b}$  is the global displacement vector,  $\mathbf{P}$  is the load vector,  $\mathbf{B}$  is the strain-displacement matrix, and  $\mathbf{D}$  is the elasticity matrix.<sup>9</sup> For the element,  $\boldsymbol{\varepsilon}$  is the strain tensor,  $\mathbf{b}^e$  is the displacement vector, and  $\boldsymbol{\sigma}$  is the stress tensor.  $\boldsymbol{\varepsilon}_0$  and  $\boldsymbol{\sigma}_0$  are initial strain and stress, which are assumed to be zero in our model.

For the plane strain problem, we have the three principle stresses ( $\sigma_{11}$ ,  $\sigma_{22}$ ,  $\sigma_{33}$ ) after Equation (S15) is solved

$$\sigma_{11} = \frac{\sigma_{xx} + \sigma_{yy}}{2} + \sqrt{\left(\frac{\sigma_{xx} - \sigma_{yy}}{2}\right)^2 + \tau_{xy}^2}, \quad (\text{S16})$$

$$\sigma_{22} = \frac{\sigma_{xx} + \sigma_{yy}}{2} - \sqrt{\left(\frac{\sigma_{xx} - \sigma_{yy}}{2}\right)^2 + \tau_{xy}^2}, \quad (\text{S17})$$

$$\sigma_{33} = \sigma_{zz} = -\mu(\sigma_{xx} + \sigma_{yy}), \quad (\text{S18})$$

where  $\sigma_{xx}$ ,  $\sigma_{yy}$ , and  $\sigma_{zz}$  are the stress components in the three directions:  $x$  (vertical direction),  $y$  (horizontal direction), and  $z$  (perpendicular to the  $xy$  plane).  $\tau_{xy}$  is the shear stress, and  $\mu$  is the Poisson's ratio. According to Tresca failure criterion, the maximum shear stress  $\tau_{\max}$  is calculated as<sup>10</sup>

$$\tau_{\max} = \frac{1}{2} \max(|\sigma_{11} - \sigma_{22}|, |\sigma_{22} - \sigma_{33}|, |\sigma_{33} - \sigma_{11}|). \quad (\text{S19})$$

For each element in the SEI layer, the material fails if the maximum shear stress is larger than the critical shear stress  $\tau_0$ , expressed as

$$\tau_{\max} \geq \tau_0. \quad (\text{S20})$$

## References

1. A. F. Voter, in *Radiation effects in solids*, Springer, 2007, pp. 1-23.
2. H. Iddir and L. A. Curtiss, *The Journal of Physical Chemistry C*, 2010, **114**, 20903-20906.
3. Y. Chen, C. Ouyang, L. Song and Z. Sun, *The Journal of Physical Chemistry C*, 2011, **115**, 7044-7049.
4. O. Borodin and D. Bedrov, *The Journal of Physical Chemistry C*, 2014, **118**, 18362-18371.
5. R. Jasinski, by P. Delahey and CW Tobias, *Interscience*, New York, 1971, **8**, 253.
6. P. Arora, M. Doyle and R. E. White, *Journal of The Electrochemical Society*, 1999, **146**, 3543-3553.
7. M. Jäckle and A. Groß, *The Journal of chemical physics*, 2014, **141**, 174710.
8. H. Carslaw and J. Jaeger, *Conduction of heat in solids: Oxford Science Publications*, Oxford, England, 1959.
9. K.-J. Bathe, *Finite element procedures*, Klaus-Jurgen Bathe, 2006.
10. R. M. Christensen, *The theory of materials failure*, Oxford University Press, 2013.